6 KIEE International Transactions on PE, 12A-1, 6-14 (2002)

A Study on Voltage Collapse Mechanism using Equivalent Mechanical Model

Do-Hyung Kim, Heon-Su Ryu, Jong-Gi Lee and Young-Hyun Moon

Abstract - In this paper, an EMM(Equivalent Mechanical Model) is developed to explain the voltage collapse mechanism by reflecting the effects of reactive powers. The proposed EMM exactly represents the voltage instability mechanism described by the system equations. By the use of the EMM model, the voltage collapse mechanism has been illustrated by showing the exactness of the results. The stable region has been investigated with a reactive-power-controlled two-bus system, which shows that special alerts are required when the system operates with leading power factor. It is also discussed a system transform technique to eliminate the resistance component of the Thevenin equivalent impedance for practical applications. Finally, the results adopting the proposed method for sample systems which were transformed are listed

Keywords - voltage collapse mechanism, equivalent mechanical model, energy function, parametric instability, maximum power transfer.

1. Introduction

The voltage stability problem is now a serious concern in large electric power systems. The continuing interconnection of bulk power system has led to experience abnormally low voltage and voltage collapse phenomena. With difficulty in expanding of electric utility due to economic and environmental limitations, the power system occasionally operates even closer to the limits of stability.

The voltage problems are related to the increased loading of transmission lines, and insufficient local reactive power supply. The voltage instability also attributed to the lack of reactive compensation or control. Voltage collapse phenomena have many complicate aspects with various time frames from several seconds to several decades of minutes. This brought about many arguments on whether the characteristics of voltage collapse is static or dynamic, system intrinsic or system-load interacting. This is because the voltage collapse mechanism is not clarified yet.

A majority of the work on the problem to date has been focused on the static problem such as load flow feasibility, optimal power flow, steady-state stability. Venikov et al. [1] suggested voltage stability based on a steady state sensitivity analysis using a simple two bus system. Kwatny et al. [2] studied the static problem as a static bifurcation of loadflow equations and illustrated how bifurcation could describe instability both in voltage and angle. Tamura et al.[3] explained the voltage collapse by multiple load flow solutions with the use of the relationships between the voltage instability and closely-located solution pair. In the modal analysis technique [5,6,7], several eigenvalues of the reduced Jacobian matrix close to the imaginary axis are intensively investigated with their eigenvectors to show the voltage collapse condition. Dobson and Chiang et al.[9] discussed about the dynamics of voltage collapse claiming that the voltage collapse results from as a dynamic consequences of the bifurcation. Although there is extensive literature on voltage collapse, very few deal with the physical mechanism of the voltage collapse phenomenon

This study attempts to develop an EMM model for the voltage collapse mechanism. Since the voltage collapse phenomenon is highly dependent on reactive powers, the EMM model is developed to reflect the effects of reactive powers by modifying the conventional model of mechanical analogy for angular stability analysis.

This study shows that the proposed EMM exactly represents the voltage instability mechanism described by the system equations. The proposed EMM model illustrates the voltage collapse mechanism to provide some intuitive physical meanings. The stable region has been investigated with a reactive-power-controlled two-bus system, which shows that special alerts are required when the system operates with leading power factor.

Finally, practical applications are discussed with the use of Thevenin's equivalent circuit for the whole power system seen from a load terminal. In this case, the Thevenin equivalent impedance has non-negligible resistance. This paper introduces a system transform technique presented in Ref.[11,12] to eliminate the resistance. Test results are listed.

2. EMM for Power Systems

Many attempts have been made to develop a visual modeling of power system for stability analysis. The me-

Manuscript received: Nov. 15, 2001 accepted: Jan. 9, 2002.

Do-Hyung Kim, Heon-Su Ryu, Jong-Gi Lee and Young-Hyun Moon are with Dept. of Electrical Engineering, Yonsei Univ., Seoul, 120-749, Korea.

chanical analogy is the well-known model to give precise concepts of the angular stability. Luders[10] suggested a mechanical analogy system for a power system and derived an energy function.

His mechanical analogy is developed with the strict restriction of constant voltage. In this paper, a mathematically exact EMM of multi-machine systems is systematically developed to apply to voltage stability analysis. In order to explain the voltage collapse phenomenon highly dependent on the reactive powers, an EMM model should be developed to reflect the effects of reactive powers. The EMM is developed first for a simple two-bus system, and later generalized to be applicable to multi-bus systems with the use of the classical generator model.

Consider the following two-bus system with a pure reactive line. The generator is assumed to be of round-rotor type. The internal reactance of the generator is considered as a part of the line impedance. The system configuration and its phasor diagram are shown in Fig. 1.

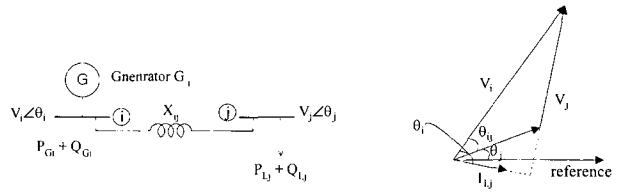

(a) System Configuration (b) V-I Phasor Diagram

Fig. 1 Two-bus System with Pure Reactive Line

The following EMM can be developed by slightly modifying the conventional spring model in order to take bus voltages as variables and to reflect reactive powers into the EMM.

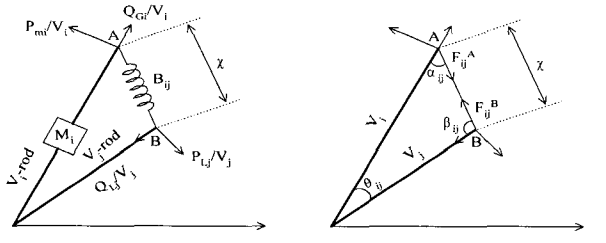

where $B_{ij} = 1./X_{ij}$
M_i : Generator Inertia
(a) EMM

where $\chi \sin\alpha_{ij} = V_j \sin\theta_{ij}$
$\chi \cos\alpha_{ij} = V_i - V_j \cos\theta_{ij}$
(b) Force Diagram

Fig. 2 Equivalent Mechanical Model

Here, it should be noted that the lengths of both rods are flexible like a pole of car antenna. Those lengths are determined by the force balance at points A and B. The lengths of V_i-rod and V_j -rod represent the voltage magnitudes at the generator and load buses respectively. The exactness of the above EMM can be verified by showing that the dynamic equations of EMM agree exactly with the power swing equations and the load flow equations for the given power system. In the above force diagram, the magnitudes of spring forces are given by

$$|\mathbf{F}_{ij}| = |\mathbf{F}_{ji}| = B_{ij}\chi \tag{1}$$

where $Bij(= 1/X_{ij})$ is the spring constant

Both of the force vectors can be represented with the directional unit vectors $\hat{\boldsymbol{\theta}}$ and $\hat{\mathbf{r}}$ as follows:

$$\begin{aligned}\mathbf{F}_{ij} &= -B_{ij}\chi\cos\alpha_{ij}\hat{\mathbf{r}} - B_{ij}\chi\sin\alpha_{ij}\hat{\boldsymbol{\theta}} \\ &= -B_{ij}(V_i - V_j\cos\theta_{ij})\hat{\mathbf{r}} - B_{ij}V_j\sin\theta_{ij}\hat{\boldsymbol{\theta}}\end{aligned} \tag{2}$$

$$\begin{aligned}\mathbf{F}_{ji} &= -B_{ij}\chi\cos\beta_{ij}\hat{\mathbf{r}} - B_{ij}\chi\sin\beta_{ij}\hat{\boldsymbol{\theta}} \\ &= B_{ij}(V_i\cos\theta_{ij} - V_j)\hat{\mathbf{r}} + B_{ij}V_i\sin\theta_{ij}\hat{\boldsymbol{\theta}}\end{aligned} \tag{3}$$

The above equations can be easily proven by using the trigonometric relations shown in Fig. 2(b). The force balance conditions at both points in the EMM give the following dynamic equations:

$$\text{Generator: } \frac{1}{V_i}\left[-M_i\ddot{\theta}_i - D_i\dot{\theta}_i + P_{mi} - V_i\,V_j\sin\theta_{ij}\right] = 0 \tag{4}$$

$$\frac{Q_{Gi}}{V_i} - B_{ij}(V_i - V_j\cos\theta_{ij}) = 0 \tag{5}$$

$$\text{Load : } \frac{P_{Lj}}{V_j} - B_{ji}V_i\sin\theta_{ji} = 0 \tag{6}$$

$$-\frac{Q_{Lj}}{V_j} - B_{ji}(V_j - V_i\cos\theta_{ji}) = 0 \tag{7}$$

Here, it can be easily checked that the first two equations describe exactly the power swing equations and reactive power constraints at Bus i, and the last two, the load flow equations at Bus j for the given power system.

The above EMM can be easily generalized for multibus systems. For example, we will consider the following three-bus system, which is the smallest system including all types of buses. The line impedance are determined to reflect the generator internal impedance by the bus elimination technique.

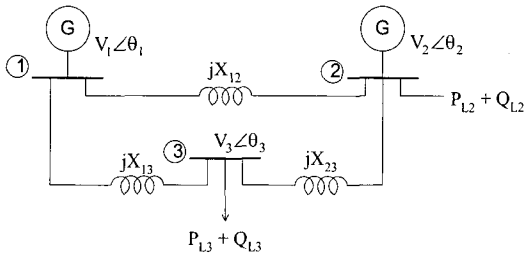

Fig. 3 Three-Bus System

By assuming $\theta_1 > \theta_2 > \theta_3$, we can obtain the following EMM for the above system with the impedance model. By observing the force diagram in Fig.4, it can be shown that the following force balance equation holds for arbitrary point i:

$$\frac{M_i\ddot{\theta}_i}{V_i}\hat{\theta} + \frac{D_i\dot{\theta}_i}{V_i}\hat{\theta} = \frac{P_{mi}\hat{\theta} - P_{Li}\hat{\theta}}{V_i} + \sum_{j\neq i} F_{ij} + \frac{Q_{Gi} + Q_{Ci} - Q_{Li}}{V_i}\hat{r} \tag{8}$$

where $i, j \in \{1,2,3\}$

Substitution of (2) into the above equation yields the following equations for each component.

$$(M_i\ddot{\theta}_i + D_i\dot{\theta}_i)/V_i - (P_{mi} - P_{Li})/V_i - \sum_{j\neq i}(-B_{ij}V_j \sin\theta_{ij}) = 0 \tag{9}$$

$$\sum_{j\neq i}[B_{ij}(V_i - V_j\cos\theta_{ij})] - (Q_{Gi} - Q_{Ci} - Q_{Li})/V_i = 0 \tag{10}$$

where $\delta_i = \theta_i$ for generator bus i

$M_i = D_i = P_{mi} = Q_{Gi} = 0$ for load bus

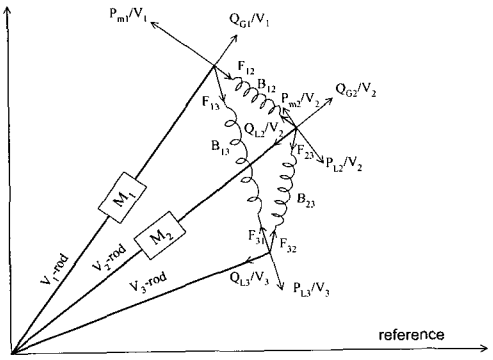

Fig. 4 EMM for Multibus System

From the above equations, it can be also easily checked that the force balance equations agree exactly with the power swing equations for a generator bus, and with real and reactive power balance equations for a load bus. The proposed EMM fully represents the system behavior of the multimachine system with the classical generator model. This implies that the voltage collapse mechanism may be visualized by the proposed EMM.

3. Visual Modeling Of Voltage Collapse Mechanism

For the visual modeling of voltage collapse mechanism, we will consider the following simple generator-load system. The generator is represented by the classical model with the round rotor type, and the load is assumed to be a constant power load.

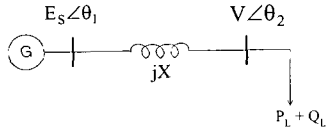

Fig. 5 Generator - Load System

In order to calculate the steady state equilibriums, we may assume the following input-output balance condition ;

$$P_m = P_L \tag{11}$$

By using (11), the following energy function can be derived from the EMM in Fig.2 in terms of ω, V and load angle θ_{12}

$$E = \frac{1}{2}M\omega^2 + \frac{1}{2}BV^2 - BE_sV\cos\theta_{12} - P_L\theta_{12} + Q_L\log(V/V_0) \tag{12}$$

where $\theta_{12} = \theta_1 - \theta_2$: load angle

B=1/X,

The above energy function has equilibrium points which can be given by the solution of the following partial equations.

$$\frac{\partial E}{\partial \omega} = 0 \Rightarrow M\omega = 0 \tag{13}$$

$$\frac{\partial E}{\partial \theta_{12}} = 0 \Rightarrow BE_sV\sin\theta_{12} - P_L = 0 \tag{14.a}$$

$$\frac{\partial E}{\partial V} = 0 \Rightarrow BV - BE_s\cos\theta_{12} + \frac{Q_L}{V} = 0 \tag{14.b}$$

The above equations are just the same as the load flow equations, which have two solutions; one high-voltage solution and the other low-voltage solution. Since the energy function(12) well reflects the system behaviors of the EMM, the equilibrium points can be visualized on the proposed EMM. This gives a hint that the proposed EMM may visualize the voltage collapse mechanism. By examining the EMM carefully, we can easily find that the proposed EMM has two equilibrium points. For the convenience of the discussion, we will consider the case where the load varies with a constant power factor.

To begin with, we examine the trajectory of the equilibrium points when the load varies with a constant power factor. Fig. 6 shows the trajectories of equilibrium points for the typical power factors. Fig.6(a) shows the case where the power factor is unity. The equilibrium points must lie on the half circle in order to make the angle between the force P_L/V and the V-rod rectangular.

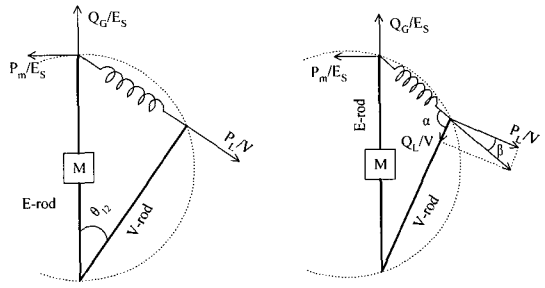

(a) pf=1.0 (b) pf = cosβ

Fig. 6 Trajectory of Equilibrium Points with Constant Power Factor

Fig. 6(b) shows the trajectory of equilibrium point when the power factor is kept to be $pf = \cos\beta$. In this case, the angle α between the spring and the V-rod should be kept

constant with $\alpha = 90^\circ + \beta$. This means that the equilibrium points must lie on an arc of a circle.

Behaviors of Equilibrium Points

With the above preliminaries, we can examine the behaviors of the equilibrium points by considering the load fluctuation with a constant power factor. As mentioned earlier, the proposed EMM has two equilibrium points as shown in Fig.7. (The equilibrium points can be obtained by solving the load flow equations.) It is noted that the dotted line must be parallel to the E-rod since both equilibrium points must satisfy

$$P_L = BE_S V_A \sin\theta_{12}^{A} = BE_S V_B \sin\theta_{12}^{B}$$

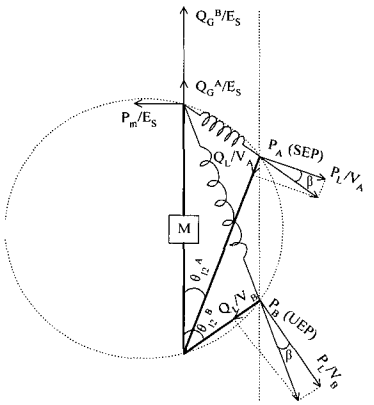

Fig. 7 Equilibrium Points of the EMM with Constant Power Factor

Say here that the load is increased by positive small perturbation ΔP_L and ΔQ_L with constant power factor for a short moment, and returns to the original load P_L and Q_L. Then, the incremental load ΔP_L and ΔQ_L will increase the length of the spring by moving the system equilibrium downward along the arc.

Assume that the system state be on the equilibrium point P_A. Then the small perturbation ΔP_L decreases the load bus voltage, where the sensitivity of the load voltage is much smaller than that of the spring length. Since the load bus voltage is high enough at the equilibrium point P_A, it is guaranteed that the forces P_L / V_A and Q_L / V_A do not change significantly. Consequently, the small load increase ΔP_L moves the system state to a new state with a little increased θ_{12}^A. If the load returns to the original load P_L in the next step, then the system naturally returns to the original state. We can say the same story with the negative ΔP_L. Therefore, the point P_A is a stable equilibrium point.

Assume in the next that the system state be on the equilibrium point P_B in Fig. 7. Then, the small increase ΔP_L in the load causes the increase in the spring length. Here it is noted that the voltage sensitivity is much greater than that of the spring length, and thus the small increase in the spring length causes a considerable reduction of the load voltage. This considerable load voltage decrease brings about a significant increase in the forces P_L / V_B and Q_L / V_B, since the voltage V_B is low enough near point P_B. Especially, the increase in the force Q_L / V_B further decrease the load voltage by directly forcing the system state to move along the arc of circle. This secondary effect to the load bus voltage accelerates the decrease of load bus voltage, which eventually results in the voltage collapse. When we have a load perturbation of negative ΔP_L, the load perturbation increase the load bus voltage with a comparatively big sensitivity. This increase in the load bus voltage reduces both forces P_L / V_B and Q_L / V_B significantly. By a similar way as given above, we can confirm that the negative ΔP_L forces the system state to move away from the low voltage equilibrium. The system state never returns to the low-voltage equilibrium after the load perturbation vanishes. Therefore, we can conclude that the low voltage equilibrium is an unstable equilibrium.

In the above discussion, we show that the proposed EMM can be utilized as a fine model to visualize the low-voltage and high-voltage solutions in static voltage analysis for the two-bus system. Here, it is noted that the above interpretation of the voltage collapse by the proposed EMM can be easily generalized for multibus systems by using the EMM as shown in Fig.4. In order to confirm that the proposed EMM can be used as an exact visual model for the voltage collapse mechanism, it is necessary to show that the EMM provides the exact voltage collapse condition with the critical voltage.

Voltage Collapse Condition on the Proposed EMM

Regarding static voltage stability analysis, the voltage collapse condition can also be derived by the use of the energy function. The energy function method [13,14] is to determine the system stability by comparing the energy difference between unstable equilibrium points(UEPs) and a stable equilibrium point(SEP). Approaching the SEP to an UEP makes the energy difference zero and brings about voltage collapse. When the SEP coalesces into an UEP, the saddle node bifurcation phenomenon occurs. Consequently, the energy function method provides the following voltage collapse condition :

$$\frac{\partial E(\mathbf{x}_e)}{\partial \mathbf{x}} = 0 \tag{15}$$

$$\left| \frac{\partial^2 E(\mathbf{x}_e)}{\partial \mathbf{x}^2} \right| = 0$$

where $\mathbf{x} = [\omega, \theta, V]^T$ (16)

Equation(15) describes the equilibrium condition of the system which yields a SEP and UEPs as the solutions. Equation(16) represents the condition that the SEP coalesces into an UEP, which can be considered as the actual voltage collapse condition. The voltage collapse condition can be visualized on the proposed EMM as shown in Fig.8.

As the load increases with the constant power factor pf=cos β , the pair of equilibrium points move to the right. The voltage collapse occurs when the SEP and UEP eventually coalesce. At this moment, the triangle in the figure becomes isosceles. By the use of the geometric relations in Fig.8, the maximum load P_{Lmax} and the critical voltage V_C can be easily calculated as follows:

$$\text{Maximum Load}: P_{L\max} = BE_S(V_c \sin\theta^c)$$
$$= BE_S(\frac{E_S}{2}\tan\theta^c)$$
$$= \frac{1}{2}BE_s^{\,2}\tan(45^\circ - \frac{\beta}{2}) \quad (17)$$

$$\text{Critical Voltage}: V_c^{\,2} + V_c^{\,2} - 2V_cV_c\cos(90^\circ+\beta) = E_s^{\,2}$$
$$\therefore V_c = \frac{E_s}{\sqrt{2}}\frac{1}{\sqrt{1+\sin\beta}} \quad (18)$$

The above results can be easily checked by comparing with those by the conventional methods (See Appendix).

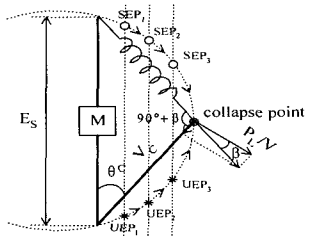

Fig. 8 Visualization of the Collapse Condition

4. Investigation Of Stable Region

The proposed EMM gives intuitive geometric relations in voltage stability analysis, which can be utilized for the practical application to the system operation. The following examples illustrate the usefulness of the proposed EMM for the operator's conceptual understanding. From now on , we will use the EMM diagram which is obtained just by omitting the masses and the springs in the original EMM.

Reactive-Power-Controlled 2-Bus System

Consider the voltage stability of 2-bus system with a capacitor bank to control the reactive power as shown in Fig.9

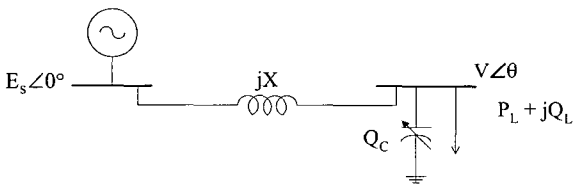

Fig. 9 Reactive-Power Controlled 2-Bus System

Case 1) When the capacitor bank has limited capacity

In this case, the load bus voltage V can be controlled to keep $V = V_S$ unless the required reactive power exceeds the maximum capacity (Q_{max}).

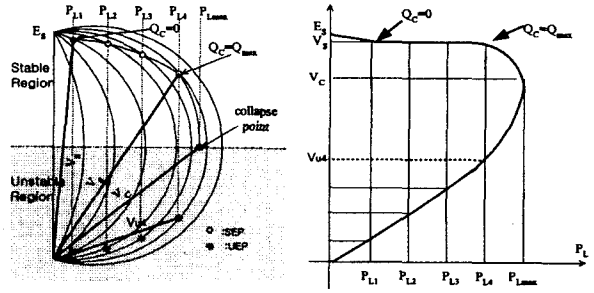

(a) EMM diagram (b) Nose Curve

Fig. 10 EMM and Nose Curve for the Q_c -Controlled System

Fig. 10(a) shows the stability region with the moves of SEP and UEP positions as the load increases. The upper half past is the stable region and the lower half part the unstable by examining Fig.10(a), we can obtain the conventional nose curve as shown in Fig.10(b). It is noted here that equilibrium points do not follow the arc for the interval $P_{L4} < P_L < P_{L\max}$. This is because the increase of load continuously changes the power factor when the capacitor bank supplies the maximum reactive power.

Case 2)When the capacity of the capacitor bank is big enough

If the capacity of the capacitor bank is big enough, the load bus voltage can be controlled to keep $V = V_S$. Consequently, we can draw the EMM diagram as given in Fig.11 to show the stability region.

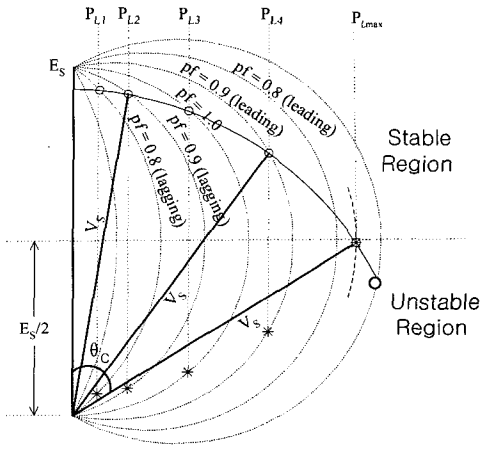

Fig. 11 EMM Diagram with a Capacitor Bank of Enough Capacity

In this case, one may think that the maximum transfer power $P_{L\max}$ calculated by (17), can be infinity since the power factor cosβ can be controlled. However, Eq.(17) is derived without considering the load bus voltage. If we

supply too much reactive power by the capacitor bank, then the load bus voltage increases too high. Therefore, it is required to keep the load voltage within the tolerance. For simplicity of discussion, we assume that load bus voltage must be kept to the specified voltage. Then, the system operating point moves alone the circle with radius V_S as the load P_L increases. Since the capacitor bank is controlled stepwise, load fluctuation makes the equilibrium points move along an arc of the circle with constant power factor. Consequently, the system has one stable equilibrium and an unstable equilibrium point for each load level. If the load increases to $P_{L\max}$, then the coalescence of SEP and UEP occurs, which directly brings about the voltage collapse. Therefore, there is still a power transfer limit even though the system has enough reactive power control capacity. The maximum power can be directly calculated from the geometric relation of the EMM diagram

$$P_{L\max} = BE_S V_S \sin\theta_L = BE_S V_S(\sqrt{V_S^2 - (E_S/2)^2}/V_S) = BE_S\sqrt{V_S^2 - E_S^2/4} \quad (19)$$

The same result can be obtained from (A.9) and (A.11) in the appendix.

For the special case where $V_S = E_S$, the maximum power transfer is given by

$$P_{L\max} = \frac{\sqrt{3}}{2}\frac{E_S V_S}{X} \quad (20)$$

It is also interesting to observe what would happen when the load is increased greater than $P_{L\max}$. In this case, we can find a solution which satisfies the load flow equation. The EMM diagram in Fig.11 shows that the solution is an unstable solution. Moreover, we can easily confirm this fact by checking the eigenvalues of the Jacobian matrix (The reactive power equation must be considered with constant Q_C since Q_C changes stepwise.). It is remarkable that the voltage collapse may occur without any indication of voltage drops when the system is operated with the leading power factor with enough reactive compensation facilities. This requires special alert in the system operation with leading power factors.

5. Applications

The voltage in stability problem can be interpreted as a complicate parametric in stability with a number of load parameters. The load parameters may vary individually. However, it is impossible to consider the individual variations of load parameters in voltage stability analysis. Instead, two approaches are commonly adopted : one is to assume that all loads vary with one load parameter for the whole system, and the other is to assume that only one load vary with all other loads remaining unchanged. For the second approach, the proposed. EMM can be a useful tool to analyze the voltage stability.

For simplicity, we assume here that all system loads be constant impedance loads and remain unchanged except the load at Bus i. Then, the system can be simplified by using Thevenin's theorem as shown in Fig.12. Thevenin equivalent voltage can be determined by using the voltage regulation ratio at the load terminal.

$$E_i^{Th} = (1+\eta_{vi}) \text{ [pu]} \quad (21)$$

with η_{vi}: voltage regulation ratio at bus i

Here it is noted that R^{Th} is not negligible since the system includes resistive loads.

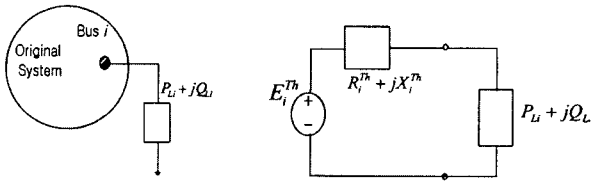

(a) Original system (b) Equivalent

Fig. 12 Thevenin Equivalent system

The equivalent system has only one transmission line to satisfy the uniform R/X ratio. Consequently, the equivalent system can be transformed to eliminate the resistance by using a method presented in Ref.[11,12]. The transformed system can be easily obtained as follows:

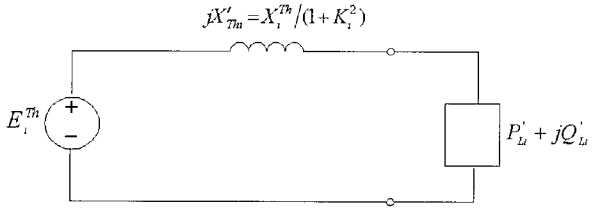

Fig. 13 Transformed System

In Fig.13, the transformed parameters are determined by

$$X'_{Thi} = X_i/(1+K_i^2) \quad (22)$$

$$P'_{Li} = P_{Li} - K_i Q_{Li} = P_{Li}(1 - K_i \tan\beta_i) \quad (23)$$

$$Q'_{Li} = Q_{Li} + K_i P_{Li} = Q_{Li}(1 + K_i \cot\beta_i) \quad (24)$$

where $K_i = R_i^{Th}/X_i^{Th}$

By using the transformed system, one can easily find that the critical voltage at bus i is determined by (18).

$$V_{Ci} = \frac{E_i^{Th}}{\sqrt{2}}\cdot\frac{1}{\sqrt{1+\sin\beta_i}} = \frac{1+\eta_{vi}}{\sqrt{2}\cdot\sqrt{1+\sin\beta_i}} \text{ [pu]} \quad (25)$$

where β_i : power factor of the load at bus i

Here it should be noted that Eq.(25) shows that the critical collapse voltage is directly related to the voltage regulation ratio. The maximum power transferred to load at bus i

can be easily calculated by using (17) as follows :

$$P_{Li}^{'\max} = \frac{1}{2} B_i^{'} (E_i^{Th})^2 \tan(45° - \frac{\beta_i}{2}) \quad (26)$$

where $B_i^{'} = 1/X_{Li}^{'Th}$

By using (23), we can calculate the actual maximum power transfer from the result of (26).

$$P_{Li}^{\max} = P_{Li}^{'\max} / (1 - K_i \tan \beta_i) \quad (27)$$

The above algorithm is tested for some of various sample systems with heavy load conditions. The results are listed in the following tables.

Table 1 Results from IEEE 14-Bus System

Bus No.	$P_L + jQ_L$	η_v	V_c	$P_{L\max}$	$P_{L\max}/P_{L0}$
1	0	0.00000	0.70711	6.17665	-
2	0.2170 + 0.1270i	0.01137	0.58284	4.36347	20.10814
3	0.9420 + 0.1900i	0.03220	0.65350	4.55709	4.83767
4	0.4780 - 0.0390i	0.00453	0.63598	4.97801	10.41425
5	0.0760 + 0.0160i	0.00260	0.63476	4.86120	63.96313
6	0.1120 + 0.0750i	0.01113	0.57311	2.41668	21.57746
9	0.2950 + 0.1660i	0.03583	0.59988	2.17976	7.38902
10	0.0900 + 0.0580i	0.01625	0.57882	1.81930	20.21449
11	0.0350 + 0.0180i	0.00619	0.58936	1.87342	53.52633
12	0.0610 + 0.0160i	0.01078	0.63821	2.02357	33.17323
13	0.1350 + 0.0580i	0.01985	0.61058	2.21791	16.42894
14	0.1490 + 0.0500i	0.02918	0.63381	1.76807	11.86623

Table 2 Results from IEEE 39-Bus System

Bus No	$P_L + jQ_L$	η_v	V_c	$P_{L\max}$	$P_{L\max}/P_{L0}$
1	0	0	0.7071	19.3558	-
3	3.2200 + 0.0240i	0.0421	0.6597	40.3553	12.5327
4	5.0000 + 1.8400i	0.1041	0.6730	40.4097	8.0819
7	2.3380 + 0.8400i	0.0529	0.6436	29.8526	12.7684
8	5.2200 + 1.7600i	0.1200	0.6895	30.4986	5.8426
12	0.4400 + 0.8800i	0.0431	0.5359	9.4285	21.4284
15	3.2000 + 1.5300i	0.0728	0.6341	38.9286	12.1652
16	3.2940 + 0.3230i	0.0475	0.6632	54.7037	16.6071
18	1.5800 + 0.3000i	0.0264	0.6498	38.5121	24.3748
20	6.8000 + 1.0300i	0.1257	0.7127	15.2467	2.2422
21	2.7400 + 1.1500i	0.0639	0.6388	25.1836	9.1911
23	2.4750 + 0.8460i	0.0547	0.6484	18.4547	7.4565
24	3.0860 - 0.9220i	0.0215	0.6467	32.0385	10.3819
25	2.2400 + 0.4720i	0.0451	0.6617	28.8351	12.8728
26	1.3900 + 0.1700i	0.0267	0.6500	25.5886	18.4090
27	2.8100 + 0.7550i	0.0611	0.6687	27.2341	9.6918
28	2.0600 + 0.2760i	0.0573	0.6694	11.6330	5.6471
29	2.8350 + 0.2690i	0.0700	0.6775	11.4367	4.0341
31	0.0920 + 0.0460i	0.0025	0.5892	10.4395	113.4729
39	11.040 + 2.5000i	0.3369	0.8464	18.9096	1.7128

The generator internal impedances are appropriately selected within 0.2 ~ 0.3 pu, and the power factors are assumed to be no greater than 0.98 in case of heavy loads to bring about the voltage collapse.

6. Conclusions

For the mechanical analogy of the voltage collapse mechanism , an EMM model is developed to reflect the effects of reactive powers. The proposed EMM exactly represents the voltage instability mechanism described by the system equations, which enables us to visualize the voltage collapse mechanism.

The two bus system with reactive control facility is thoroughly examined by the use of the EMM, which shows that the voltage collapse may occur without any indication of voltage drops when the system is operated with leading power factor, which require special alerts in system operations. Finally, practical applications are discussed with introduction of a system transform technique to eliminate the resistance in the Thevenin equivalent circuit seen from the load terminal concerned.

References

[1] Venikov, V.A. Stroev, V.I. Idelchick and V.I. Tarasov, " Estimation of Electric Power System Steady-state Stability in Load Flow Calculations," IEEE Trans. on PAS, Vol. PAS-94, No.3, pp. 1034-1041, May 1975.

[2] H.G. Kwatny, A.K.Pasrija and L.Y. Bahar, "Static Bufurcations in Electric Power Networks: Loss of Steady-State Stability and Voltage Collapse," IEEE Trans. on Power Systems, Vol.5, No.1, pp. 198-203, Feb. 1990.

[3] Y. Tamura, H. Mori and S. Iwamoto, "Relationship Between Voltage Instability and Multiple Load Flow Solutions in Electric Power Systems,", IEEE Trans. on Power Apparatus and Systems, Vol. PAS-102, No.

5, May 1983.

[4] R.A. Schlueter, I. Hu, M.W. Chang and J.C. Lo, A. Costi, "Methods for Determining Proximity to Voltage Collapse," IEEE Trans. on Power Systems, Vol.6, No.1, pp. 285-292, Feb. 1991.

[5] B. Gao, G.K. Morison and P.O. Kundur, "Voltage Stability Evaluation Using Modal Analysis," IEEE Trans. on Power Systems, Vol. 7, No. 4, November 1992

[6] N. Flatabe, R. Ognedal and T. Carlsen, "Voltage Stability Condition in a Power Transmission System Calculated by Sensitivity Methods," IEEE Trans. on Power Systems, Vol. 5, No. 4, November 1990.

[7] P.A. Lof, T. Smed, G. Anderson and D.J. Hill, "Fast Calculation of a Voltage Stability Index," IEEE Trans. on Power Systems, Vol. 7, No. 1, February 1992.

[8] Claudio A and Ca~nizares,"On Bifurcation, Voltage Collapse and Load Modeling," IEEE Trans. on Power Systems, Vol.10 ,No. 1 pp. 512-522, Feb. 1995.

[9] I.Dobson, H.D. Chiang, R.J.Thomas, J.S.Thorp and L.Fekih-Ahmed, "On voltage collapse in electric power systems", IEEE Trans. on Power Systems, vol. 5, No 2, May. 1990, pp.601-611.

[10] G. A. Luders, "Transient Stability of Multimachine Power Systems via the Direct Method of Lyapunov," IEEE Trans. Power App.Syst., Vol. PAS-90, NO.1, p.23-35, JAN/FEB 1971.

[11] Y.H. Moon, E.H. Lee and T.H. Roh, "Development of an Energy function Reflecting the Transfer Conductance foe Direct Stability Analysis in Power Systems", IEE Proc.-Gener. Transm. Distrib., Vol. 144, No. 5, pp. 503-509, 1997.9.

[12] Y.H. Moon, B.H. Cho, T.H. Rho and B.K. Choi, "The Development of Equivalent System Technique for Deriving an Energy Function Reflecting Transfer Conductances," IEEE Trans. on Power Systems, Vol.14, No.4, pp.1335-1341, November 1999.

[13] N. A. Tsolas, A. Arapostathis and P. P. Varaiya,"A Structure Preserving Energy Function for Power System Transient Stability Analysis," IEEE Trans. on Circuit and Systems, Vol. CAS-32, NO.10, p.1041-1049, October 1985.

[14] A. R. Bergen and D. J. Hill, "A Structure Preserving Model for Power System Stability Analysis," IEEE Trans. Power App. Syst., Vol. PAS-100, NO.1, p.25-33, January 1981.

[15] C.L. DeMarco and T. J. Overbye, "An Energy Based Security Measure for Assessing Vulnerability to Voltage Collapse, " IEEE Trans. on Power Systems, Vol.5, No.2, pp. 419-426, May 1990.

[16] T. J. Overbye and C. C. DeMarco, "Improved Techniques for Power System Voltage Security Assessment Using Energy Methods, "IEEE Trans. on Power System, Vol.6. NO.4, pp. 1446-1452, Dec 1991.

[17] Y.H. Moon, "A New Approach to Derive an Energy Integral for the Direct method of Stability Analysis in Power Systems," Journal of Electrical Eng. and Information science, Vol.1, No.1, p.58-69, March, 1996.

[18] Y.H. Moon and E.H. Lee, "On the Identity of Static Voltage Stability Analysis Method in Power Systems," IASTED International Conference, April 1995.

[19] Y.H. Moon and E.H. Lee, " Visualization of Voltage Collapse Mechanism by the Direct Method based on EMM," IASTED/ISMM International Conference, April 1996.

[20] Y.H. Moon, B.K. Choi and B.H. Cho, "Estimation of Maximum Loadability in Power Systems By Using Elliptic Properties of P-e Curve" IEEE WM 99', p.677-682.

APPENDIX : Analysis of Voltage Collapse Condition

This appendix provides analysis of voltage collapse condition for a 2-bus system given in Fig.5 by using various approaches. It is assumed that the load varies with constant power factor, that is

$$\tan\beta = \frac{Q_L}{P_L} = \frac{dQ_L}{dP_L} \tag{A.1}$$

For a 2-bus system, the elimination of variable θ_{12} from the load flow equations yields

$$P_L{}^2 + \left(Q_L + BV^2\right)^2 = B^2 E_S{}^2 V^2 \tag{A.2}$$

Sensitivity Analysis

From (A.2),we can obtain the following derivative :

$$\frac{dV}{dP_L} = \frac{P_L + \left(Q_L + BV^2\right)\tan\beta}{2B^2V\left[\frac{E_S{}^2}{2} - \frac{Q_L}{B} - V^2\right]} \tag{A.3}$$

The voltage collapse condition that $dV/dP_L = \infty$ in the sensitivity analysis gives

$$\frac{E_S{}^2}{2} = V^2 + \frac{Q_L}{B} \tag{A.4}$$

In order to get the critical load, we can eliminate Q_L and V from (A.2) by using (A.1) and (A.4), which yields

$$P_L{}^2 + BE_S{}^2 \tan\beta P_L - \frac{B^2 E_S{}^4}{4} = 0 \tag{A.5}$$

Equation (A.5) gives the following critical load (or maximum load)

$$\begin{aligned} P_{L\max} &= -\frac{1}{2}BE_S{}^2\tan\beta + \frac{1}{2}BE_S{}^2\sqrt{1+\tan^2\beta} \\ &= \frac{1}{2}BE_S{}^2\left(\frac{1-\sin\beta}{\cos\beta}\right) \\ &= \frac{1}{2}BE_S{}^2\tan\left(45^\circ - \frac{\beta}{2}\right) \end{aligned} \tag{A.6}$$

Successive substitution of (A.1) and (A.6) into (A.4) yields the following critical voltage

$$V_C = \frac{E_S}{\sqrt{2}}\sqrt{1-\tan\left(45°-\frac{\beta}{2}\right)\tan\beta}$$
$$= \frac{E_S}{\sqrt{2}}\frac{1}{\sqrt{1+\sin\beta}} \quad (A.7)$$

Both of the results (A.6) and (A.7) agree with (17) and (18) derived by the EMM approach

Energy Function Approach

The collapse condition(16) by the energy function gives

$$M\left[BE_S V\cos\theta_{12}\left(B-\frac{Q_L}{V^2}\right)-\left(BE_S\sin\theta_{12}\right)^2\right]=0 \quad (A.8)$$

By using the load flow equations, (A.8) can be rewritten as

$$B^2V^4 = P_L{}^2 + Q_L{}^2 = \left(1+\tan^2\beta\right)P_L{}^2$$
$$\therefore\ BV^2 = \frac{P_L}{\cos\beta} \quad (A.9)$$

By eliminating Q_L and V in (A.2) with the use of (A.1) and (A.9), we can obtain

$$\frac{1}{\cos^2\beta}P_L{}^2 + 2B\frac{\tan\beta}{\cos\beta}P_L{}^2 + \frac{1}{\cos^2\beta}P_L{}^2 = \frac{BE_S{}^2}{\cos\beta}P_L \quad (A.10)$$

By solving (A.10), we can easily calculate the maximum load as follows :

$$P_{L\max} = \frac{\cos\beta}{1+\sin\beta}\frac{BE_S{}^2}{2}$$
$$= \frac{1}{2}BE_S{}^2\left(\frac{1-\sin\beta}{\cos\beta}\right) \quad (A.11)$$

By substituting (A.7) into (A.9), we can obtain the following critical voltage

$$V_C = \frac{E_S}{\sqrt{2}}\frac{\sqrt{1-\sin\beta}}{\cos\beta}$$
$$= \frac{E_S}{\sqrt{2}}\frac{1}{\sqrt{1+\sin\beta}} \quad (A.12)$$

The above results also agree with those by the proposed EMM approach. It can be found in the literature[18] that all of the various approaches to voltage stability analysis are based on the unique identity of the system.

Young-Hyun Moon was born in Korea, on March 11, 1952. He received B.S and M.S. degrees in Electrical Engineering from Seoul National University, and the M.S. and Ph.D. degrees from Oregon State University in 1975, 1978, 1980, and 1983, respectively. In 1983, he joined the faculty of Yonsei University, Seoul, Korea, and is now a professor of Electrical Engineering. He visited Univ. of Illinois for the 1992-1993 academic year. Dr. Moon is a member of the IEEE Power Engineering Society. His specialization is state estimation, system control, and stability analysis in electric power systems.

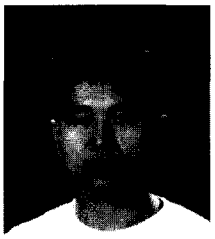

Do-Hyung Kim was born in Korea, on May 30, 1971. He received B.S degree in Civil Engineering from Korea Military Academy in 1993 He is currently pursuing a M. S. degree in Electrical Engineering at Yonsei University. His research interests are in the area of voltage stability analysis.

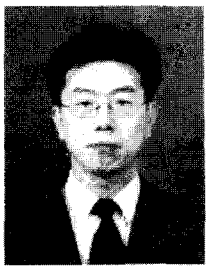

Heon-Su Ryu was born in Korea, on June 03, 1969. He received B.S and M.S. degrees in Electrical Engineering from Yonsei University, Korea, in 1992, and 1996, respectively. He is currently pursuing a Ph.D. degree in Electrical Engineering at Yonsei University. Mr. Ryu is a student member of the IEEE Power Engineering Society. His research interests are in the area of stability analysis and control of power system.

Jong-Gi Lee was born in Korea, on Dec. 12, 1971. He received B.S degree in Electrical Engineering from the University of Suwon in 1997 and M.S. degree in Electrical Engineering from Yonsei University, Korea in 1999. He is currently pursuing a Ph.D. degree in Electrical Engineering at Yonsei University. His research interests are in the area of stability analysis and state estimation.